

## SYNTHESIS, CHARACTERIZATION AND PHOTOVOLTAIC APPLICATION OF SILVER DOPED CdS/PVA NANOCOMPOSITE THIN FILMS

D. SAIKIA<sup>\*</sup>, P. K. SAIKIA<sup>b</sup>, P. K. GOGOI<sup>a</sup>, P. SAIKIA<sup>b</sup>

*Material Science Laboratory, Department of Physics, Sibsagar College, Joysagar 785665, India.*

*<sup>a</sup>Center for Nanoscience and Composite Materials, Department of Chemistry, Dibrugarh University, Dibrugarh-786004, India.*

*<sup>b</sup>Department of Physics, Dibrugarh University, Dibrugarh-786004, India*

CdS quantum dot(QD) embedded in PVA matrix were prepared in thin film form on chemically cleaned glass substrates by dip coating technique followed by direct heat treatment of the substrate. The synthesis method reported in this study is free from ammonia. Silver was doped into CdS/PVA thin film by adding silver nitrate into cadmium acetate with cadmium to silver ion ratio 10<sup>3</sup>:1. The films were characterized by XRD, SEM, TEM, and UV-Visible and photoluminescence spectroscopy. The results indicated that films were nanocrystalline in nature, highly transparent, homogeneous with no visible pinholes and suitable for solar cell application. A CdS(PVA)/CdTe thin films solar cell using this deposition technique have been fabricated. Doping of silver into CdS/PVA nanocomposite thin film has improved the conversion efficiency of the cell from 4.92% to 5.63%.

(Received February 1, 2011; accepted April 5, 2011)

**Keywords:** Photovoltaic, CdS/PVA; Nanocomposite; Thin film, Silver doping; Solar cell; CdS(PVA)/CdTe

### 1. Introduction

In recent years, nanostructured CdS thin films has attracted wide attention as one of the most promising materials for applications as window layers [1, 2] in low-cost, high-efficiency thin film solar cells because of its suitable band gap, high optical transparency and absorption coefficient in the visible range of solar spectrum. CdS is a direct band gap (2.42 eV) II-VI semiconductor and has been used as a vital component in different solar cell heterostructures together with narrow band gap materials such as CdTe, Cu<sub>2</sub>S, InP, CuInSe<sub>2</sub> with efficiencies between 10-16 % [3,4].

Among all thin film polycrystalline CdTe based solar cells, (CdS/CdTe) exhibit the highest efficiency of 16.5% [5] and this value was achieved by using chemically deposited CdS thin films. In recent years high priority has been given to develop low cost deposition technique for CdS thin films [1]. Though various deposition techniques such as thermal evaporation [6], spray pyrolysis [7], laser evaporation [8], electro-deposition [9,10] and solid state reaction[11] technique have been reported the chemical bath deposition (CBD) technique appears to be most suitable because of simplicity, easy to handle, cost effective and wide industrial applications.

Recently, doped CdS nanostructures has attracted attention not only because of their tunable optical and electrical properties [12] but also due to inherent potential for many technological applications such as wavelength controlled lasers [13] and solar cells [14]. Several

---

\*Corresponding author: dulen.s@rediffmail.com

cations such as Hg, In, Mn, Cu, Ag [15-17] were used for doping CdS by various methods. Optical properties including fluorescence of CdS doped with Cu, Ag and Au have been studied in detail. The defect in the structure of Ag doped CdS were reported by Vidyanath et al. [18]. M.A. Khalid et al. [19] reported the electrical and optical properties of polycrystalline Ag doped CdS thin films prepared by spray pyrolysis technique. Influence of Cu doping on the optoelectronic properties of chemically deposited CdS thin film were reported by D. Petre et al. [20]. Muneeb et al. [21] reported that silver impurity reduces the resistivity of CdS thin film and changes the type of the semiconductor from n-type to p-type. X. Li. et al. [22] reported that Ag doping induces change in crystal structure of CdS thin film from cubic to hexagonal.

Furthermore, solar cells incorporating semiconductor quantum dots and organic polymers may provide lightweight, flexible and cheaply produced alternative to the conventional bulk semiconductor solar cells. Quantum dot (QD) solar cells have the potentials to increase the maximum conversion efficiency of solar photon up to 66% [23] by utilizing photogenerated carriers to produce higher photovoltages or photocurrent. In principle, there are three different QD solar cell configurations; these are (i) Photo-electrodes composed of quantum dot arrays, (ii) QD-sensitized nanocrystalline TiO<sub>2</sub> solar cell and (iii) cells with QDs employed as light absorbers and component of charge transport networks. The power conversion efficiencies in these devices are currently very low due to limitations arising mainly from charge transport inefficiencies. Existing polymer based organic photovoltaic devices are currently limited to the solar power conversion efficiencies of 3-5%. Still there is enough room for further research in this field for the improvement of the efficiency of QD based solar cells.

Normally, for obtaining CdS thin film by CBD technique an aqueous solution of cadmium salt is used as a source of Cd ion and thiourea as the source of sulfur in presence of a base, e.g., ammonia [24] or ethylenediamine [25,26] or EDTA [27] as a complexing agent. In the present study we report an ammonia free synthesis of CdS quantum dot (QD) in PVA matrix grown from a solution containing Cd:S in the ratio 3:5 by dip coating technique followed by direct heating of the substrate. The structural, morphological and optical properties of the films were investigated by XRD, SEM, TEM, UV-Vis and photoluminescence spectroscopy. Two thin film solar cells with the structures CdS(PVA)/CdTe and Ag:CdS (PVA)/CdTe have been fabricated using this deposition technique. The photovoltaic parameters of the cells were compared.

## **2. Experimental**

### **2.1 Chemicals**

All reagents were of analytical grade, obtained from Merk(India) Ltd. and used as received without further purification. Deionized water was used throughout the experiments.

### **2.2 Synthesis of CdS/PVA and Ag:CdS/PVA nanocomposite thin films:**

CdS/PVA nanocomposite thin films were deposited on glass substrates by CBD technique using cadmium acetate  $[(\text{CH}_3\text{COO})_2\text{Cd} \cdot 2\text{H}_2\text{O}]$  as Cd<sup>++</sup> ion source and thiourea  $[\text{CS}(\text{NH}_2)_2]$  as S<sup>2-</sup> ion source with cadmium to sulfur ratio: (Cd:S) 3:5 and polyvinyl alcohol (PVA) as a polymer controller matrix. The Cd:S ratio plays an important role on the structure of the CdS thin film because S-excess and Cd-excess films exhibit hexagonal and cubic structure, respectively [28]. For solar cell application hexagonal films are preferable. In a typical reaction a matrix solution was prepared by adding 20 ml of 0.6 M cadmium acetate into an equal volume of 5% aqueous solution of polyvinyl alcohol (PVA) and stirred continuously for 90 minutes at 70 °C. The solution was left overnight to get transparent liquid indicating complete dissolution of cadmium acetate. To this matrix solution, 20 ml of 1 M thiourea was added dropwise and the reactants were stirred continuously for 30 minutes. For the preparation of CdS/PVA nanocomposite thin film, a chemically clean glass substrate was coated with the sol by dip coating technique and then the

substrate was heated in an oven at 100°C. Within 15-20 minutes the colour of the film changed from transparent to light yellow indicating the formation of CdS/PVA nanocomposite thin film. For the preparation of Ag:CdS/PVA nanocomposite thin film, 20  $\mu$ l of 0.6 M silver nitrate solution was added to 20 ml of 0.6 M of cadmium acetate solution prior to the formation of the matrix and proceeded as described above.

### 2.3 Characterization

For optical studies, optical absorption and transmission spectra were recorded with a Scinco(S-3100) PD UV-Vis spectrophotometer. Photo-luminescence spectra were recorded with a HORIBA JOBIN-YVON Fluoromax-4 spectrofluorometer. Surface morphology of the films was examined by LEO 1430VP Scanning Electron Microscope. The high resolution transmission electron microscopy (HRTEM) images were taken by TECNAI-30 model instrument operated at an accelerating voltage of 300 kV.

## 3. Results and discussion

### 3.1 Optical studies

The absorption spectra of CdS/PVA and Ag-doped CdS/PVA nanocomposite thin films prepared at 100°C are shown in Fig.1 (a). From the spectra it is evident that the absorbance edges are blue shifted with respect to the bulk CdS(520 nm), indicating quantum confinement effect in nanoparticles. The absorption spectra of Ag-doped CdS/PVA thin film shows a maximum at around 425 nm, and compared with undoped CdS/PVA thin film (450 nm), 25 nm blue shift was observed. This might be due to the formation of smaller sized nanoparticles when silver impurity was doped into the pure CdS/PVA thin film. Fig.1 (b) shows the plot of  $(Ahv)^2$  versus photon energy  $hv$  for the undoped and Ag-doped CdS/PVA film. The optical band gaps of the films were obtained by using the following equation [29] for a semiconductor

$$A = K ( hv - E_g )^{m/2} / hv \quad (1)$$

where ‘A’ is the absorbance, ‘K’ is a constant and ‘m’ is equal to 1 for direct transition and 2 for indirect transition . Linearity of the plots indicates that the material is of direct band gap nature. The extrapolation of the straight line to  $(Ahv)^2 = 0$  axis gives the energy band gap of the film material [29]. The band gap was found to increase from 2.562 eV for undoped CdS/PVA film to 2.736 eV for Ag-doped CdS/PVA film. From the band gap information the size of the CdS nanoparticles were calculated using the effective mass approximation (EMA) method and following the equation [30] for a semiconductor. They are tabulated in Table 1.

$$E_{gn} - E_{gb} = [ (h^2 \pi^2 / 2R^2) 1/m^* ] \quad (2)$$

In the above equation  $m^*$  is the effective mass of the specimen,  $E_{gb}$  is the bulk band gap(2.42 eV) and  $E_{gn}$  is the calculated band gap of the sample (Table 1).

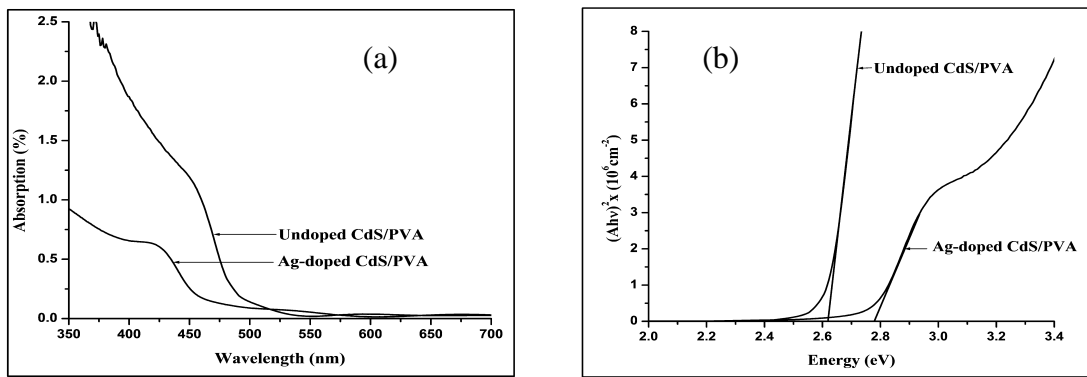


Fig.1 (a) UV-visible absorption spectra and (b) plot of  $(A(hv))^2$  versus photon energy ( $h\nu$ ) and wavelength for undoped and Ag-doped CdS/PVA nanocomposite thin films prepared at 100°C.

*Table. 1: Particle size from band gap information.*

Sample	Band gap from UV-Vis (eV)	Shift in band gap (eV)	Grain size from EMA (nm)
CdS/PVA	2.61	0.19	6.25
Ag:CdS/PVA	2.78	0.36	4.54

Fig 2 (a) shows the plot of wavelength versus transmittance for CdS/PVA and Ag-doped CdS/PVA nanocomposite thin films deposited at 100°C. Both the films show more than 90% transmission for wavelength greater than 500 nm. The sharp fall in transmission near the fundamental absorption edge is indicative of the good crystallinity of the films

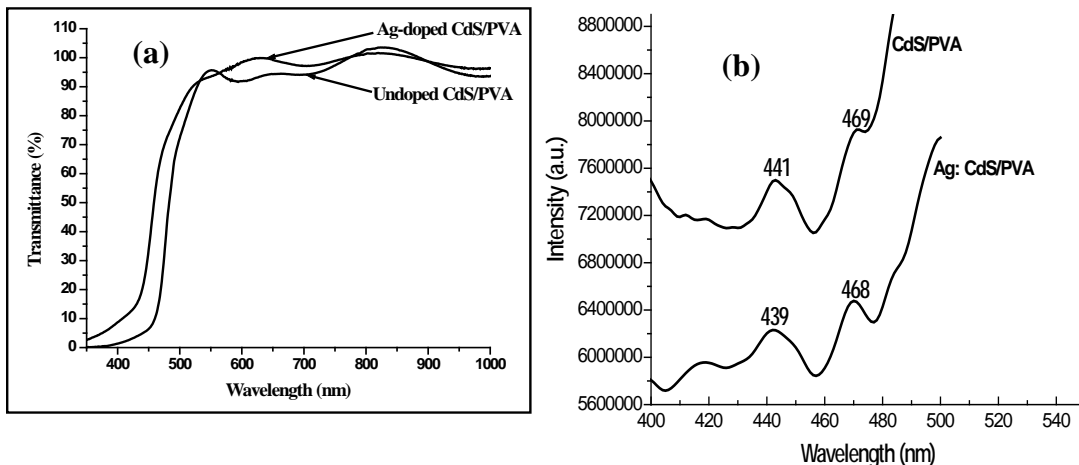


Fig. 2 (a) Transmittance (a) and (b) PL spectra of un-doped and Ag-doped CdS/PVA nanocomposite thin film versus wavelength for films prepare at 100 °C.

The rise and fall in transmittance for wavelengths greater than 500 nm may be attributed to the interference of light transmitted through the thin film and the substrate [30]. A little increase

in transmittance was observed for the film doped with silver in the wavelength range 550 nm to 700 nm. A similar increase in transmittance was also observed by D. Petre et al. [20] in CdS thin film after Cu doping.

The formation of CdS nanoparticles can also be confirmed by photo-luminescence (PL) spectroscopy, as CdS nanoparticles exhibit light emitting behavior at specific wavelength [31, 32]. Fig. 2(b) shows the PL spectra of the CdS/PVA and Ag-doped CdS/PVA nanocomposite thin films prepared at 100°C and excited at 350 nm. The observed results show that there are two distinct peaks which are situated at 440 nm (broad emission) and 468 nm (narrow emission), respectively. The emission peak centered at 468 nm was found more prominent in Ag-doped CdS/PVA thin film as compared to undoped CdS/PVA thin film.

### 3.2 Surface morphology

The Scanning Electron Micrographs of as deposited CdS/PVA and Ag doped CdS/PVA nanocomposite thin films are shown in Fig.3 (a) and 3(b). The surface morphology clearly shows that the film is almost homogeneous, without any pinholes or cracks and covered the substrate well. From the micrographs it is observed that the particle size in CdS/PVA thin film decreases after doping with silver. Fig.3 (c) shows the X-ray diffraction curves of undoped and Ag-doped films. There is observed a large peak that demonstrates the major nanostructure of the films, while small narrow peaks are a proof for minor microcrystalline phases formed in the film matrix.

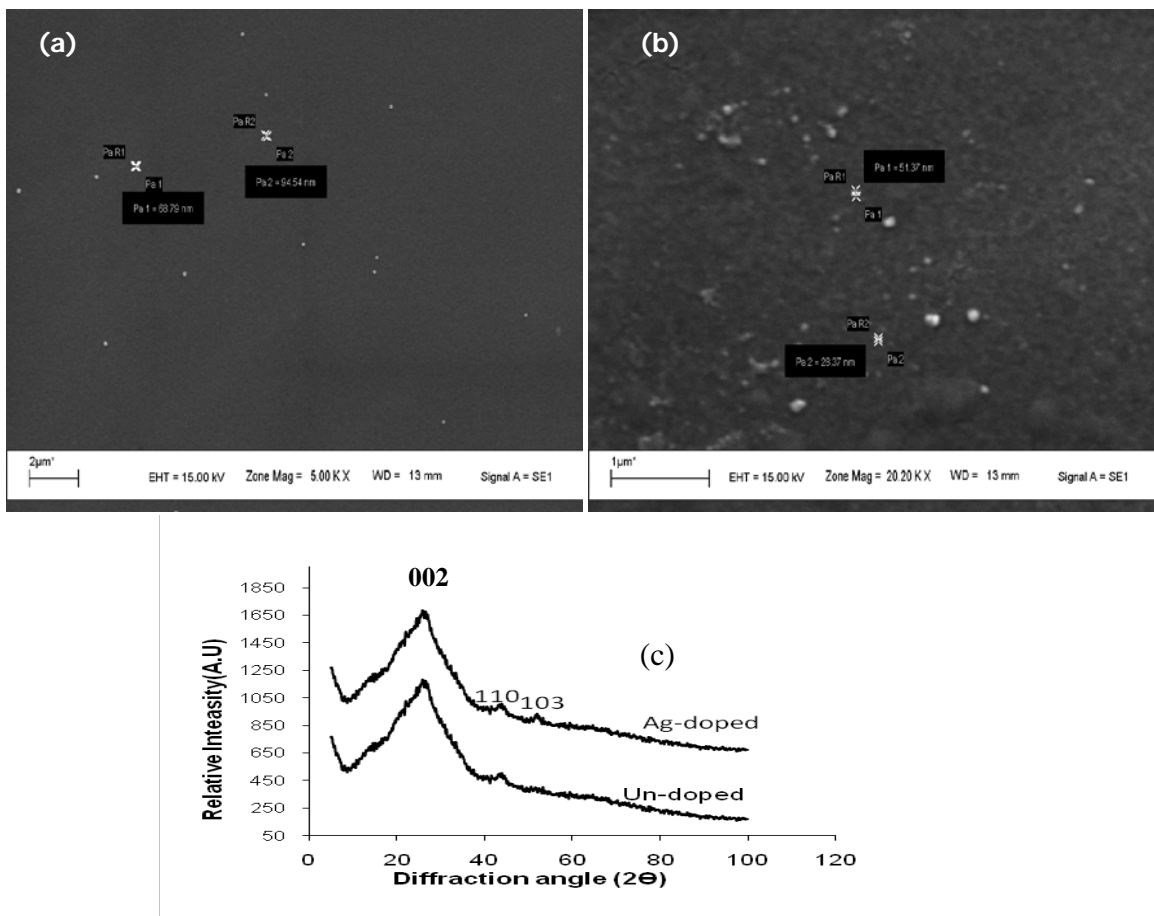


Fig. 3 The SEM images of (a) CdS/PVA and (b) X-ray diffraction curves of Ag:CdS/PVA nanocomposite thin films deposited 100 °C.

### 3.3 TEM analysis

The transmission electron microscopy (TEM) images of CdS/PVA and Ag:CdS/PVA nanocomposite thin films deposited at 100°C are shown in Fig. 4(a) and 4(b). Fig. 4(c) shows the high resolution transmission electron microscopy (HRTEM) image of CdS/PVA nanocomposite thin film deposited at 100°C. The HRTEM image of the film shows the lattice fringes indicating the formation of good nanocrystalline structure. The HRTEM gives a grain size of 5 nm (Fig.4 (e)) and this is in agreement with results obtained from effective mass approximation (EMA) calculation. This confirms the formation of a nanocrystalline CdS/PVA composite thin film with particle size situated in the quantum dot range. Fig. 4(d) shows the hexagonal pattern of as synthesized CdS nanocrystallites in CdS/PVA thin film.

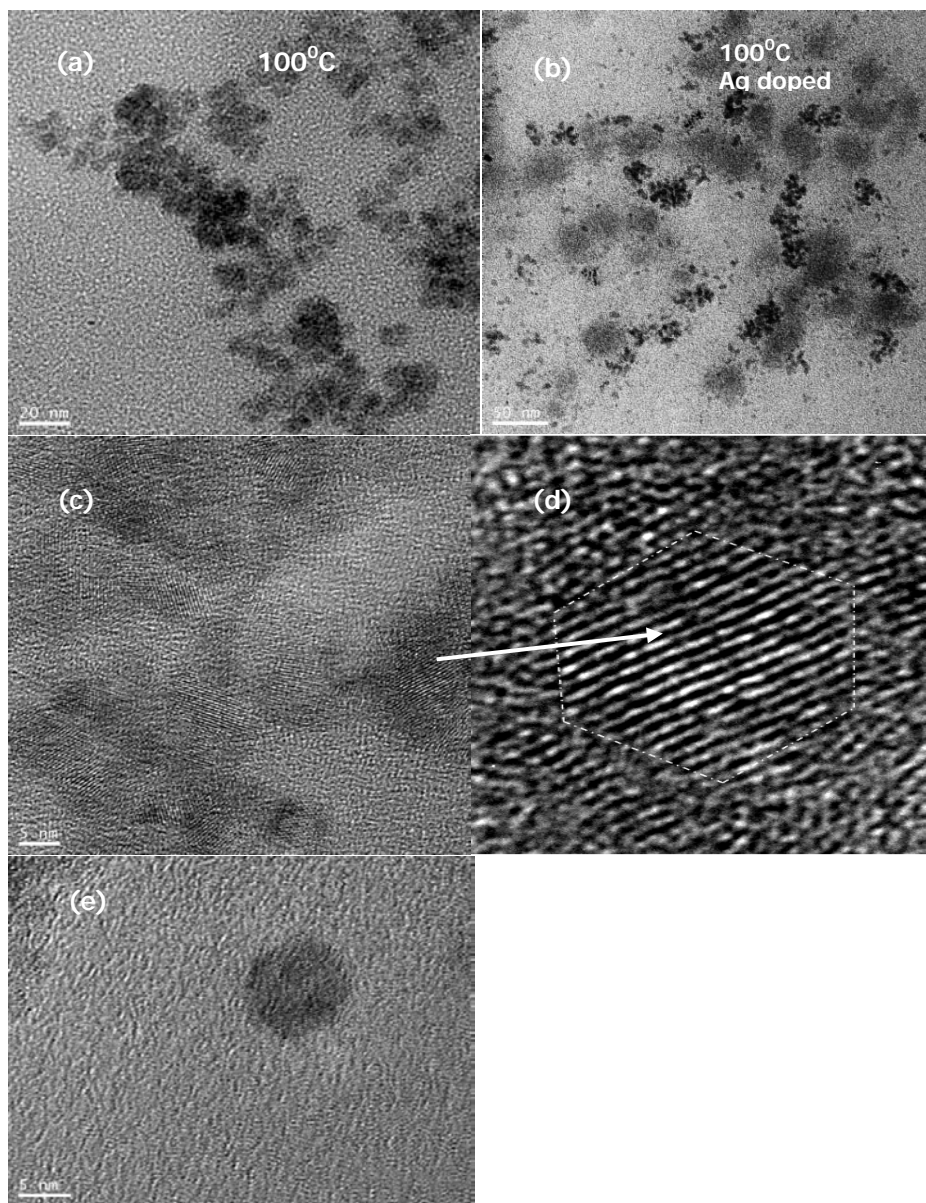


Fig. 4 : TEM picture of (a) CdS/PVA and (b) Ag:CdS/PVA thin film prepared at 100°C, (c) HRTEM image of CdS/PVA thin films (d) Hexagonal pattern of CdS nanocrystal. (e) CdS quantum dot of size  $\approx$  5 nm

#### 4. Device fabrication and characterization

Two solar cells viz. CdS(PVA)/CdTe (cell C1) and Ag:CdS(PVA)/CdTe (cell C2) were fabricated using this deposition technique for CdS/PVA and Ag:CdS/PVA nanocomposite thin films. The structures of the cells are shown in Fig.5(a). The CdS:PVA/CdTe and Ag:CdS/PVA thin film solar cells fabricated in this study are made up of four layers. First the glass substrate was covered by ~210 nm thick layer of transparent conducting oxide (TCO) which in our case is tin oxide ( $\text{SnO}_2$ ). The CdS/PVA or Ag:CdS(PVA) nanocomposite thin film was then deposited on the top of TCO to a thickness of approximately 100 nm by the method as described above. Before deposition of CdTe, CdS/PVA or Ag:CdS(PVA) film was annealed for 15 minutes at  $100^{\circ}\text{C}$ . A layer of CdTe of thickness ~ 870 nm was then thermally evaporated on the top at a base pressure  $< 10^{-6}$  mbar. Before making the top contact, CdTe was treated with  $\text{CdCl}_2$  at  $200^{\circ}\text{C}$  in a tube furnace for one hour under ambient conditions. The  $\text{CdCl}_2$  treatment is important because it improves the crystalline quality of CdTe by increasing the size of small grains and by removing several defects in the material. After  $\text{CdCl}_2$  treatment, CdTe was etched in a mixture of nitric acids and phosphoric acid to avoid the formation of unwanted  $\text{CdO}$  or  $\text{CdTeO}_3$  on CdTe surface in order to make good contact on CdTe. Finally, a layer of HgTe was deposited on the top as a back contact by thermal evaporation method at a pressure  $< 10^{-6}$  mbar. The device had an area of  $1 \times 1 \text{ cm}^2$  and found stable for several months.

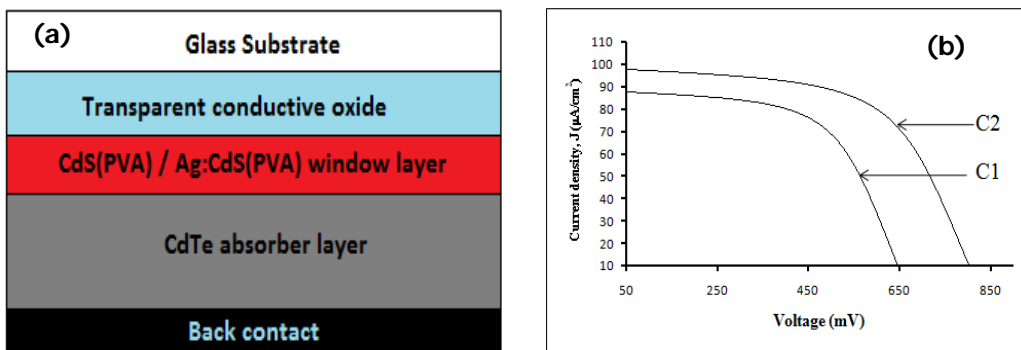


Fig. 5 (a) Structure and (b) I-V characteristics of CdS(PVA)/CdTe and Ag:CdS(PVA)/CdTe heterojunction solar cell

The current-voltage(I-V) characteristics of the cells C1 (CdS(PVA)/CdTe) and C2 (Ag:CdS(PVA)/CdTe) were measured with a high impedance ( $\sim 10^{14}$ ) ECIL electrometer amplifier (model EA812) and is shown in Fig. 5(b). The intensity of illumination was measured with a Lutron LX-101 lux meter. The solar cell parameters were measured under illumination with a  $50 \text{ mW Cm}^{-2}$  (0.5 SUN) tungsten lamp. The observed photovoltaic parameters of the cells are tabulated in Table 2. A conversion efficiency of 4.92% ( $V_{oc} = 0.617 \text{ V}$ ,  $J_{sc} = 87 \mu\text{A}/\text{cm}^2$ , FF = 0.63) has been achieved for the cell C1 and it was found to increase to 5.63% ( $V_{oc} = 0.797 \text{ V}$ ,  $J_{sc} = 98 \mu\text{A}/\text{cm}^2$ , FF = 0.71) for the cell C2 in which the CdS window layer was doped with silver. The cell doped with silver showed an increase in efficiency from 4.95 to 5.8 % against its undoped counterpart.

Table. 2: Current –Voltage parameters for the cells C1 and C2 under  $50 \text{ mWcm}^{-2}$  illumination intensity

Solar Cell	$I (\text{mW Cm}^{-2})$	$V_{oc} (\text{mV})$	$J_{sc} (\mu\text{A Cm}^{-2})$	FF (%)	$\eta (\%)$
C1: CdS(PVA)/CdTe	<b>50</b>	<b>617</b>	<b>87</b>	<b>63.0</b>	<b>4.92</b>
C2: CdS(PVA)/CdTe	<b>50</b>	<b>797</b>	<b>98</b>	<b>71.0</b>	<b>5.63</b>

The parameters shown are the open circuit voltages ( $V_{oc}$ ), short circuit current density ( $J_{sc}$ ), fill factor (FF) and efficiency ( $\eta$ ).

## 5. Conclusions

In summary, CdS quantum dot (QD) embedded in PVA matrix in thin film form have been synthesized by dip coating technique from an ammonia free bath. The effect of silver doping on the optical and photovoltaic properties of CdS/PVA thin film has also been reported. The as prepared films were found to be nanocrystalline in nature. The particle size of CdS embedded in PVA matrix of  $\sim 5 \text{ nm}$ ; in the quantum dot range, as calculated from absorption spectra using effective mass approximation (EMA) method was in reasonably good agreement with those obtained from HRTEM. The efficiency of CdS(PVA)/CdTe solar cell was found to increase from 4.92% to 5.63% after silver doping.

Further study will focus on the improvement of the conversion efficiency of the cell.

## Acknowledgement

The authors acknowledge CIF, Indian Institute of Technology, Guwahati, North East Institute of Science and Technology, Jorhat, and National Chemical Laboratory, Pune for recording SEM, XRD and HRTEM. One of the authors D. Saikia, acknowledges UGC, New Delhi for financial support under CPE scheme to Sibsagar College, Joysagar.

## References

- [1] G. Sasikala, P. Thilakan, C. Subramanium Sol. Energy Mater. Sol. Cells **62**, 275 (2000).
- [2] S.A. Mahmoud, A.A. Ibrahim, A.S. Raid, Thin Solid Films **372**, 144 (2000).
- [3] A. Romeo, D.L. Batzner, H. Zoog, C.Vignali, A.N. Tiwari, Sol. Energy Mater. Sol. Cells **67**, 311 (2001).
- [4] A. Kylner, J. Appl. Phys. **85**, 6858 (1999).
- [5] Xuanzhi Wu, Solar Energy **77**, 803–814 (2004)
- [6] S.A. Mahmoud, A.A. Ibrahim, A.S. Raid, Thin Solid Films **372**, 144 (2000).
- [7] S. J. Castillo, A.Mendoza-Galvan, R. Ramirez-Bon, F.J. Espinoza-Beltran, M. Sotelo-Lerma, J.Gonzalez-Hernandez, G.Martinez, Thin Solid Films **373**, 10 (2000).
- [8] X.W. Wang, F.Spitulnik, B.Campell, R.Noble, R.P. Hapanowicz, R.A. Condrate Sr, L.P.Fu, A.Peteou, Thin Solid Films **218**, 157 (1992).
- [9] K.L. Choy, B.Su, Thin solid Films **388**, 9 (2001).
- [10] J.M. Nel, H.L. Gaigher, F.D. Auret, Thin Solid Films **436**, 186 (2003).
- [11] W. Wang, Z. Liu, C. Zheng, C. Xu, Y. Liu, G. Wang, Materials Letter **57**, 2755 (2003).
- [12] Y. Cui, C.M. Lieber, Science **291**, 851 (2001).
- [13] V.I. Klimov et al., Nature **447**, 441 (2007).
- [14] Ilan Gur, N.A. Fromer, M.L. Geier, A.P. Alivisator, Science 310, **462** (2005).
- [15] J. Krustok, P.E. Kukk, Mater. Sci. **15**(3), 43 (1989).

- [16] J. Krustok, J.Madasson, M. Altosaar, P. Kukk, *J. Phys. Chem.Solids* **51**(9) 1013(1990).
- [17] S. Chandramohan, A. Kanjilal, J. K. Tripathi, S. N. Sarangi, R. Sathyamoorthy, and T. Som, *J. Appl. Phys.* **105**, 123507 (2009)
- [18] H.R. Vidyanath, F.A. Kroger, *J. Phys. Chem. Solids* **36**, 509-520 (1975)
- [19] M. A. Khalid, H.A. Jassem, *Acta Physica Hungarica* **73**(1), 29-34 (1993)
- [20] D. Petre, I. Pintilie, E. Pentia, I. Pintilie, T. Botila, *Material science and Engineering* **B58**, 238-243 (1999)
- [21] M.U. Rehman, A.K.S. Aqili, M. Shafique, Z. Ali, A. Maqsood, *Journal of Material Science Letters* **11**,127 (2003).
- [22] X. Li, Y. Yin and X. Dong, *Proc. Int. Conf. Solid Dielectrics* 270-273 (2007).
- [23] Ross RT, Nozik AJ. *J Appl Phy* **53**, 3813-3818. (1982)
- [24] F.I. Ezema, S.C. Ezugwu, R.U. Osuji, P.U. Asogwa, B.A. Ezekoye, A.B.C. Ekwealor, M.P. Ogbu, *Journal of Nano-oxide glasses* **11**, 45-50 (2010)
- [25] I. S. Elashmawi, N.A. Hakeem, M.Soleman Selim, *Material Chemistry and Physics* **115**, 132 (2009) -135.
- [26] M.D. Archbold, D.P. Halliday, K.Durose, T.P.A. Hase, D.S Boyle, S.Mazzamuto, N. Romeo, A.Bosio, *Thin Solid Films* **515**, 2954 (2007).
- [27] A.V. Feitosa, M.A.R. Miranda, J.M. Sasaki, M.A. Araujo-Silva, *Brazilian Journal of physics* **34-2B**, 656 (2004).
- [28] V. Loryuenyong, N. Ruankul, N.Supso, P. Chunpadungsuk, *International Journal of Nanoscience* **7**, 279 (2008).
- [29] B. Subramanian, C. Sanjeevviraja, M. Jayachandran, *J. Cryst. Growth* **234**, 421(2002).
- [30] P. P. Sahay, R.K. Nath, and S. Tewari, *Cryst. Res. Technol.* **42**(3), 275 (2007).
- [31] Ju-Young Kim, Hong-Mo Koo, Kyo-Jin Ihn, Kyung-Do Suh, *Journal of Industrial and Engineering Chemistry* **15**, 103-109(2009).
- [32] H. Wang, P. Fang, Z. Chen, S. Wang *Applied Surface Science* **253**, 8495 (2007).